Determination of the Generalized Scattering Matrix of an Antenna From Characteristic Modes

Yoon Goo Kim and Sangwook Nam

***Abstract*—A method to determine the generalized scattering matrix of an antenna using characteristic modes is presented. When the characteristic currents flowing at a feed point, the radiation patterns of the characteristic currents, and the eigenvalues are known, the generalized scattering matrix can be calculated. It is shown that an antenna whose behavior is dominated by a single characteristic mode becomes a minimum scattering antenna. The formula is verified using a two wavelength dipole antenna and a bow-tie antenna.**

***Index Terms*—Generalized scattering matrix, minimum scattering antenna, theory of characteristic modes.**

I. Introduction

The generalized scattering matrix has long been used to analyze antennas. For example, the generalized scattering matrix was used to determine a mutual coupling among antennas [1]–[3]. In the present communication, we derive a new formula to calculate the generalized scattering matrix of an antenna using the theory of characteristic modes. The theory of characteristic modes was first developed by Garbacz [4] and was later refined by Harrington and Mautz [5]–[7]. The theory of characteristic modes is helpful in the analysis of electromagnetic scattering problems.

A minimum scattering (MS) antenna is one that does not scatter electromagnetic fields at all when its antenna ports are terminated in suitable reactive loads [8]. An MS antenna that does not scatter when its antenna ports are open-circuited is called a canonical minimum scattering (CMS) antenna [8]. Rogers demonstrates that lossless antennas whose scattering behavior is dominated by a single characteristic mode can be MS antennas [9]. In his study, there is no condition that determines when an MS antenna becomes a CMS antenna. In the present communication, we find the conditions under which an antenna becomes either an MS or a CMS antenna in the cases of both lossy and lossless antennas.

Finally, we validate the formula by calculating the generalized scattering matrices of a two wavelength dipole antenna and a bow-tie antenna.

II. Spherical Wave and Generalized Scattering Matrix

Electric fields $\mathbf{E}$ and magnetic fields $\mathbf{H}$ in a source-free region can be expressed as a superposition of spherical waves:

$$\mathbf{E} = \sum_{s=1}^{2}\sum_{n=1}^{\infty}\sum_{m=-n}^{n} Q_{s,m,n}^{(c)}\mathbf{E}_{s,m,n}^{(c)} = k\sqrt{\eta}\sum_{s=1}^{2}\sum_{n=1}^{\infty}\sum_{m=-n}^{n} Q_{s,m,n}^{(c)}(-1)^m\mathbf{F}_{s,m,n}^{(c)} \tag{1a}$$

$$\mathbf{H} = \sum_{s=1}^{2}\sum_{n=1}^{\infty}\sum_{m=-n}^{n} Q_{s,m,n}^{(c)}\mathbf{H}_{s,m,n}^{(c)} = \frac{jk}{\sqrt{\eta}}\sum_{s=1}^{2}\sum_{n=1}^{\infty}\sum_{m=-n}^{n} Q_{s,m,n}^{(c)}(-1)^m\mathbf{F}_{3-s,m,n}^{(c)} \tag{1b}$$

where k is the wavenumber, η is the intrinsic impedance, $Q_{s,m,n}^{(c)}$ is the complex amplitude of the spherical wave, and $\mathbf{F}_{s,m,n}^{(c)}$ is defined as in [2, p. 13]. In the present communication, the $e^{j\omega t}$ time convention is used. (c, s, m, n) are the indices of the spherical waves. $s = 1$ denotes the TE mode, and $s = 2$ denotes the TM mode. $c = 1$ denotes standing waves, $c = 3$ denotes incoming waves, and $c = 4$ denotes outgoing waves. A standing wave consists of an incoming wave and an outgoing wave, and the relationship among the standing wave, incoming wave, and outgoing wave is

$$\mathbf{E}_{s,m,n}^{(1)} = \frac{1}{2}\mathbf{E}_{s,m,n}^{(3)} + \frac{1}{2}\mathbf{E}_{s,m,n}^{(4)} \tag{2a}$$

$$\mathbf{H}_{s,m,n}^{(1)} = \frac{1}{2}\mathbf{H}_{s,m,n}^{(3)} + \frac{1}{2}\mathbf{H}_{s,m,n}^{(4)}. \tag{2b}$$

The complex amplitude of the outgoing spherical wave, $Q_{s,m,n}^{(4)}$, is determined from the current distribution using the following formula [2, p. 333]:

$$Q_{s,m,n}^{(4)} = -(-1)^m \int_V \left(\mathbf{E}_{s,-m,n}^{(1)}\cdot\mathbf{J} - \mathbf{H}_{s,-m,n}^{(1)}\cdot\mathbf{M}\right) dv \tag{3}$$

where $\mathbf{J}$ is the electric current density, $\mathbf{M}$ is the magnetic current density, and V is the region enclosing all sources. The ordering of spherical waves used in this communication is the same as that used in [2].

Amplitudes of incident and reflected waves on the feed waveguide of an antenna and amplitudes of incoming and outgoing spherical waves are related by the following generalized scattering matrix equation [2]:

$$\left[\begin{array}{c} w \\ \hline \mathbf{b} \end{array}\right] = \left[\begin{array}{c|c} \Gamma & \mathbf{R} \\ \hline \mathbf{T} & \mathbf{S} \end{array}\right]\left[\begin{array}{c} v \\ \hline \mathbf{a} \end{array}\right] \tag{4}$$

where v is the amplitude of an incident wave at the feed waveguide and w is the amplitude of a reflected wave at the feed waveguide. $\mathbf{a}$ is an infinite-dimensional column matrix containing the amplitudes of the incoming spherical waves, and $\mathbf{b}$ is an infinite-dimensional column matrix containing the amplitudes of the outgoing spherical waves for the total field (scattered field + incident field). Γ is the reflection coefficient, and $\mathbf{T}$, $\mathbf{R}$, and $\mathbf{S}$ describe, respectively, the transmitting, receiving, and scattering properties of antennas. The wave functions are normalized such that one-half of the square of the absolute value of the amplitude is the power carried by the wave.

The receiving pattern of a reciprocal antenna can be determined from the transmitting pattern. $\mathbf{R}$ is determined using the following equation [2, p. 36]:

$$R_{s,m,n} = (-1)^m T_{s,-m,n} \tag{5}$$

where $T_{s,m,n}$ and $R_{s,m,n}$ are the elements of $\mathbf{T}$ and $\mathbf{R}$, respectively, and the subscripts denote the indices of the spherical waves.

III. Theory of Characteristic Modes

In this section, we briefly summarize the theory of characteristic modes. The theory of characteristic modes is extensively described in previous studies [5]–[7]. An operator equation describing a scattering of bodies is

$$T(f) = g^i \tag{6}$$

where

$$T = \begin{bmatrix} Z & N \\ N & Y \end{bmatrix}, \quad f = \begin{bmatrix} \mathbf{J} \\ j\mathbf{M} \end{bmatrix}, \quad g^i = \begin{bmatrix} \mathbf{E}^i \\ j\mathbf{H}^i \end{bmatrix}. \tag{7}$$

Here, $\mathbf{E}^i$ is an incident electric field or tangential component of an incident electric field, and $\mathbf{H}^i$ is an incident magnetic field or the tan-

Manuscript received September 09, 2012; revised April 18, 2013; accepted June 03, 2013. Date of publication July 04, 2013; date of current version August 30, 2013. This work was supported by the Korea Communications Commission (KCC), under the R&D program supervised by the Korea Communications Agency (KCA) (KCA-2011-11911-01110).

The authors are with the Department of Electrical Engineering and Computer Science, Seoul National University, Seoul 151-742, Korea (e-mail: scika@ael.snu.ac.kr; snam@snu.ac.kr).

Color versions of one or more of the figures in this communication are available online at http://ieeexplore.ieee.org.

Digital Object Identifier 10.1109/TAP.2013.2269763

gential component of an incident magnetic field. We use the tangential component where surface or line currents are present. Z, Y, and N are obtained after formulating an integro-differential equation.

There are two types of eigenvalue equation that determine the characteristic modes when bodies are lossy [7]. In one eigenvalue equation, the characteristic fields are orthogonal. In the other eigenvalue equation, the eigenvalues and eigenvectors are real. The eigenvalue equation for which the eigenvalues and eigenvectors are real is as follows:

$$R(f_n) = \lambda_n X(f_n) \tag{8}$$

where

$$R = \frac{1}{2}(T + T^*), \quad X = \frac{1}{2j}(T - T^*) \tag{9}$$

$$f_n = \begin{bmatrix} \mathbf{J}_n \\ j\mathbf{M}_n \end{bmatrix}. \tag{10}$$

The eigenvector f_n is called the characteristic current, and the field produced by the f_n is called the characteristic field. The characteristic modes are ordered according to $|\lambda_1| \leq |\lambda_2| \leq |\lambda_3| \leq \cdots$.

The symmetric product is defined as

$$\langle f, g \rangle = \int_V (\mathbf{J} \cdot \mathbf{E} - \mathbf{M} \cdot \mathbf{H}) dv \tag{11}$$

where

$$g = \begin{bmatrix} \mathbf{E} \\ j\mathbf{H} \end{bmatrix}. \tag{12}$$

The characteristic currents are normalized such that

$$\langle f_n, R(f_n) \rangle = 1. \tag{13}$$

The total current on an antenna can be represented by a linear combination of all characteristic currents:

$$f = \sum_{n=1}^{\infty} \frac{\alpha_n f_n}{1 + j\lambda_n} \tag{14}$$

where α_n is the modal excitation coefficient and is determined by

$$\alpha_n = \langle f_n, g^i \rangle = \int_V (\mathbf{J}_n \cdot \mathbf{E}^i - \mathbf{M}_n \cdot \mathbf{H}^i) dv. \tag{15}$$

For the eigenvalue equation for which the characteristic fields are orthogonal, (14) and (15) are also valid.

IV. Formula for Generalized Scattering Matrix of Antennas

Fig. 1 shows a representation of the type of antenna addressed in this communication. The material body of an antenna is composed of conductors, dielectrics, or magnetic materials. The material body can be lossy. We assume that the material is linear and reciprocal. Moreover, we assume that the antenna is excited at an infinitesimal gap on the conducting wire and that the number of feed gaps is one. A feed waveguide is connected to a feed gap, and an antenna port is connected to the end of the waveguide (Fig. 1). Throughout this communication, we assume that a reference plane is at the feed gap and that only one mode exists in the feed waveguide.

We first consider the generalized scattering matrix of bodies without a feed gap. In this case, w, v, Γ, $\mathbf{T}$, and $\mathbf{R}$ in (4) are eliminated, and $\mathbf{a}$, $\mathbf{b}$, and $\mathbf{S}$ remain. Because the incident wave is finite at the coordinate origin, the incident wave can be expanded in terms of the standing spherical waves. Let the standing spherical wave with indices (s, m, n) be incident on a body and let its amplitude be $2a_{s,m,n}$, i.e., let $2a_{s,m,n}\mathbf{E}^{(1)}_{s,m,n}$ and $2a_{s,m,n}\mathbf{H}^{(1)}_{s,m,n}$ be incident on a body. Using

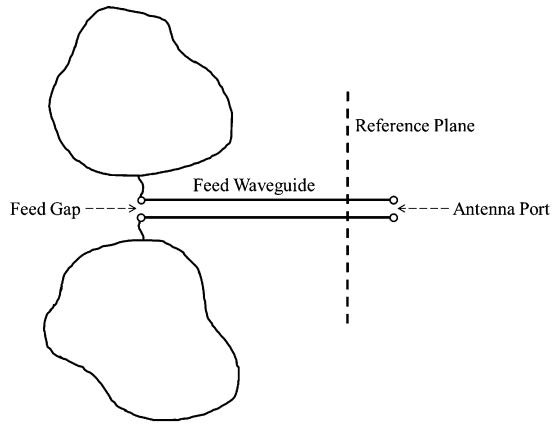

Fig. 1. Material body, feed gap, feed waveguide, reference plane, and antenna port for an antenna.

(15), the modal excitation coefficient for the pth characteristic current is given by

$$\alpha_p = 2a_{s,m,n} \int_V \left(\mathbf{J}_p \cdot \mathbf{E}^{(1)}_{s,m,n} - \mathbf{M}_p \cdot \mathbf{H}^{(1)}_{s,m,n} \right) dv. \tag{16}$$

Let the amplitude of the outgoing spherical wave with indices (s, m, n) produced by the pth characteristic current f_p be $T^p_{s,m,n}$, i.e.,

$$T^p_{s,m,n} = -(-1)^m \int_V \left(\mathbf{J}_p \cdot \mathbf{E}^{(1)}_{s,-m,n} - \mathbf{M}_p \cdot \mathbf{H}^{(1)}_{s,-m,n} \right) dv. \tag{17}$$

Comparing (16) with (17), we notice that

$$\alpha_p = -2(-1)^m T^p_{s,-m,n} a_{s,m,n}. \tag{18}$$

When multiple spherical waves are incident, the amplitudes of the incoming and outgoing spherical waves are to be represented by a column matrix $\mathbf{a}$. In this case, the modal excitation coefficient for the pth characteristic current is, from (18),

$$\alpha_p = -2\mathbf{R}^p \mathbf{a} \tag{19}$$

where $\mathbf{R}^p$ is a row matrix and the elements of $\mathbf{R}^p (R^p_{s,m,n})$ are defined by

$$R^p_{s,m,n} = (-1)^m T^p_{s,-m,n}. \tag{20}$$

Let $T^p_{s,m,n}$ be contained in a column matrix $\mathbf{T}^p$. The order of $T^p_{s,m,n}$ and the order of $R^p_{s,m,n}$ are the same as the order of the spherical waves with indices (s, m, n). When the incoming and outgoing waves with amplitude $\mathbf{a}$ are incident, the amplitudes of the outgoing spherical waves for the scattered field $(\mathbf{b}^s)$ are, from (14) and (19),

$$\mathbf{b}^s = \sum_{p=1}^{\infty} \frac{-2\mathbf{R}^p \mathbf{a}}{1 + j\lambda_p} \mathbf{T}^p. \tag{21}$$

Therefore, the amplitudes of the outgoing spherical waves for the total field $(\mathbf{b})$ when $\mathbf{a}$ is incident are as follows:

$$\mathbf{b} = \mathbf{a} - 2 \sum_{p=1}^{\infty} \frac{1}{1 + j\lambda_p} \mathbf{T}^p \mathbf{R}^p \mathbf{a} \tag{22}$$

Next, we consider the generalized scattering matrix of an antenna that has a feed gap. An antenna whose feed gap is short-circuited can be considered a body without a feed gap. If a feed gap is short-circuited,

$$w = -v. \tag{23}$$

Substituting (23) into (4) and manipulating the result, we have

$$\mathbf{b} = \left(-\frac{1}{1+\Gamma}\mathbf{TR} + \mathbf{S}\right)\mathbf{a}. \tag{24}$$

Comparing (24) with (22), we obtain

$$\mathbf{S} = \mathbf{I} + \frac{1}{1+\Gamma}\mathbf{TR} - 2\sum_{p=1}^{\infty}\frac{1}{1+j\lambda_p}\mathbf{T}^p\mathbf{R}^p \tag{25}$$

where $\mathbf{I}$ is the unit matrix.

If we excite the feed gap of an antenna with V volts, the modal excitation coefficient for the pth characteristic current is, using (15),

$$\alpha_p = VI_p \tag{26}$$

where I_p is the electric current flowing at a feed point for the pth characteristic current. From (14) and (26), the current density on the antenna when V volts are applied at the feed gap is

$$\begin{bmatrix}\mathbf{J}\\ \mathbf{M}\end{bmatrix} = \sum_{p=1}^{\infty}\frac{VI_p}{1+j\lambda_p}\begin{bmatrix}\mathbf{J}_p\\ \mathbf{M}_p\end{bmatrix}. \tag{27}$$

In this case, the amplitudes of the outgoing spherical waves that the antenna transmits ($\mathbf{b}^t$) are

$$\mathbf{b}^t = \sum_{p=1}^{\infty}\frac{VI_p}{1+j\lambda_p}\mathbf{T}^p. \tag{28}$$

If a wave with an amplitude of 1 is incident at the feed waveguide, the voltage at the feed gap is $V = \sqrt{Z_0}(1+\Gamma)$ where Z_0 is the characteristic impedance of the feed waveguide. Therefore, the $\mathbf{T}$ in (4) is

$$\mathbf{T} = \sum_{p=1}^{\infty}\frac{\sqrt{Z_0}(1+\Gamma)I_p}{1+j\lambda_p}\mathbf{T}^p. \tag{29}$$

The reflection coefficient also can be determined from the characteristic modes. From (27), the electric current at the feed point is

$$I = \sum_{p=1}^{\infty}\frac{V(I_p)^2}{1+j\lambda_p}. \tag{30}$$

Therefore, the input admittance of the antenna Y_{in} is

$$Y_{in} = \frac{1}{Z_0}\frac{1-\Gamma}{1+\Gamma} = \sum_{p=1}^{\infty}\frac{(I_p)^2}{1+j\lambda_p}. \tag{31}$$

From this equation, we can obtain the reflection coefficient.

In summary, the generalized scattering matrix can be obtained from characteristic currents at a feed point, the amplitudes of the spherical waves produced by characteristic currents, and the eigenvalues.

V. Minimum Scattering Antenna

In this section, we find the conditions under which an antenna becomes an MS antenna. We assume that the eigenvalues of the higher-order modes are very large compared with the eigenvalue of the lowest-order mode so that the currents on the antenna and the input admittance are dominated by the lowest-order mode only, i.e., $1/(1+j\lambda_1) \gg 1/(1+j\lambda_p)$, $I_1/(1+j\lambda_1) \gg I_p/(1+j\lambda_p)$, and $(I_1)^2/(1+j\lambda_1) \gg (I_p)^2/(1+j\lambda_p)(p = 2, 3, 4, \cdots)$. In this case, from (29), $\mathbf{T}$ becomes

$$\mathbf{T} \approx \frac{\sqrt{Z_0}(1+\Gamma)I_1}{1+j\lambda_1}\mathbf{T}^1. \tag{32}$$

From (5), $\mathbf{R}$ becomes

$$\mathbf{R} \approx \frac{\sqrt{Z_0}(1+\Gamma)I_1}{1+j\lambda_1}\mathbf{R}^1, \tag{33}$$

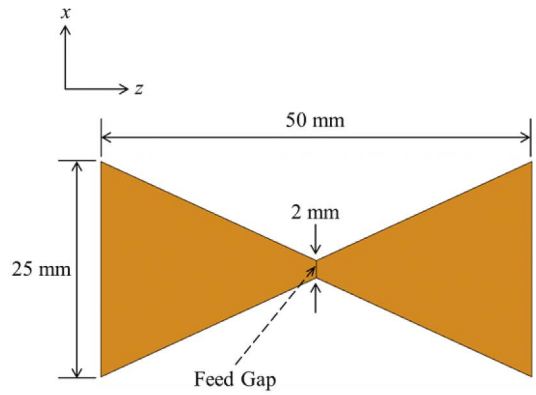

Fig. 2. Bow-tie antenna. The origin of the coordinate system is at the center of the bow-tie antenna.

and from (25), $\mathbf{S}$ becomes

$$\mathbf{S} \approx \mathbf{I} + \frac{1}{1+\Gamma}\mathbf{TR} - \frac{2}{1+j\lambda_1}\mathbf{T}^1\mathbf{R}^1. \tag{34}$$

After substituting (32) and (33) into (34) and rearranging the result,

$$\mathbf{S} \approx \mathbf{I} + \frac{1}{1+\Gamma}\mathbf{TR} - \frac{2(1+j\lambda_1)}{Z_0(1+\Gamma)^2(I_1)^2}\mathbf{TR}. \tag{35}$$

From (31), the input impedance of the antenna Z_{in} is

$$Z_{in} = Z_0\frac{1+\Gamma}{1-\Gamma} \approx \frac{1+j\lambda_1}{(I_1)^2}. \tag{36}$$

Substituting (36) into (35) and rearranging the result, we have

$$\mathbf{S} \approx \mathbf{I} - \frac{1}{1-\Gamma}\mathbf{TR}. \tag{37}$$

According to [10, eq. (16)], (37) is the same expression for $\mathbf{S}$ as that of CMS antennas. Therefore, an antenna whose behavior is dominated by a single characteristic mode and whose antenna port is at a feed gap becomes a CMS antenna.

If the antenna port is separate from a feed gap, an antenna dominated by a single characteristic mode becomes an MS antenna because a reactive load should be connected to the antenna port for the load seen at a feed gap to be an open-circuit.

VI. Validation

To verify the theory, we calculated the $\mathbf{S}$-matrix in (4) using two different methods and compared the two results. In one method, each spherical wave was incident on an antenna with a load whose impedance value was the same as the characteristic impedance of a feed waveguide. Next, we calculated the amplitudes of scattered spherical waves generated by induced currents on an antenna and used this to determine the $\mathbf{S}$. In another method, we calculated the $\mathbf{S}$ from characteristic modes using the formula presented in this communication.

We simulated two antennas. The first example is a dipole antenna with length of 300 mm and diameter of 1 mm. The conductivity of the wire was 10^5 S/m. The wire was on the z axis, and the center of the dipole was located at the origin of the coordinate system. The feed gap was at the center of the dipole antenna, and a waveguide with a characteristic impedance of 500 Ω was connected to the feed gap. The simulated frequency was 2 GHz, which gave a dipole length of 2 wavelengths. The second example is a bow-tie antenna. The bow-tie antenna was made of copper, and the size of the bow-tie antenna was shown in Fig. 2. The bow-tie antenna was fed at its center, and the characteristic impedance of the feed waveguide was 100 Ω. The simulated frequency was 3 GHz.

	TM_{01}	TM_{02}	TM_{03}	TM_{04}	TM_{05}	TM_{06}	TM_{07}	TM_{08}
TM_{01}	$0.3612+0.5039j$	0	$0.0937+0.1111j$	0	$0.2277-0.0053j$	0	$0.0680-0.0058j$	0
TM_{02}	0	$0.5147+0.6524j$	0	$0.4116+0.0410j$	0	$0.2295-0.0490j$	0	$0.0462-0.0132j$
TM_{03}	$0.0937+0.1111j$	0	$0.7351+0.5088j$	0	$-0.1766+0.2670j$	0	$-0.0431+0.0610j$	0
TM_{04}	0	$0.4116+0.0410j$	0	$-0.0508+0.5541j$	0	$-0.5009+0.2385j$	0	$-0.0968+0.0448j$
TM_{05}	$0.2277-0.0053j$	0	$-0.1766+0.2670j$	0	$0.8252+0.0802j$	0	$-0.0473+0.0084j$	0
TM_{06}	0	$0.2295-0.0490j$	0	$-0.5009+0.2385j$	0	$0.7578+0.1047j$	0	$-0.0470+0.0194j$
TM_{07}	$0.0680-0.0058j$	0	$-0.0431+0.0610j$	0	$-0.0473+0.0084j$	0	$0.9869-0.0021j$	0
TM_{08}	0	$0.0462-0.0132j$	0	$-0.0968+0.0448j$	0	$-0.0470+0.0194j$	0	$0.9909+0.0035j$

Fig. 3. S-matrix of the dipole antenna obtained using two methods, which give almost the same results.

	TE_{-11}	TM_{-11}	TM_{01}	TE_{11}	TM_{11}	TE_{-12}	TM_{-12}	TM_{02}	TE_{12}	TM_{12}
TE_{-11}	$0.9981-0.0024j$	$0.0000-0.0000j$	$-0.0001-0.0000j$	$-0.0019-0.0024j$	$-0.0000+0.0000j$	$-0.0000+0.0000j$	$0.0434-0.0017j$	$-0.0000+0.0000j$	$-0.0000+0.0000j$	$-0.0434+0.0017j$
TM_{-11}	$-0.0000+0.0000j$	$0.9891-0.0972j$	$0.0001+0.0001j$	$-0.0000+0.0000j$	$0.0109+0.0972j$	$-0.0316+0.0031j$	$-0.0000-0.0000j$	$-0.0000-0.0000j$	$-0.0316+0.0031j$	$0.0000+0.0000j$
TM_{01}	$0.0001+0.0000j$	$0.0001+0.0001j$	$0.2722+0.3965j$	$0.0001+0.0000j$	$-0.0001-0.0001j$	$-0.0000-0.0000j$	$-0.0001+0.0001j$	$0.0001-0.0002j$	$-0.0000-0.0000j$	$0.0001-0.0001j$
TE_{11}	$-0.0019-0.0024j$	$0.0000-0.0000j$	$-0.0001-0.0000j$	$0.9981-0.0024j$	$-0.0000+0.0000j$	$-0.0000+0.0000j$	$0.0434-0.0017j$	$-0.0000+0.0000j$	$-0.0000+0.0000j$	$-0.0434+0.0017j$
TM_{11}	$0.0000-0.0000j$	$0.0109+0.0972j$	$-0.0001-0.0001j$	$0.0000-0.0000j$	$0.9891-0.0972j$	$0.0316-0.0031j$	$0.0000+0.0000j$	$0.0000+0.0000j$	$0.0316-0.0031j$	$-0.0000-0.0000j$
TE_{-12}	$-0.0000+0.0000j$	$0.0316-0.0031j$	$0.0000+0.0000j$	$-0.0000+0.0000j$	$-0.0316+0.0031j$	$0.9990+0.0019j$	$-0.0000+0.0000j$	$-0.0000+0.0000j$	$-0.0010+0.0019j$	$0.0000-0.0000j$
TM_{-12}	$-0.0434+0.0017j$	$-0.0000-0.0000j$	$-0.0001+0.0001j$	$-0.0434+0.0017j$	$0.0000+0.0000j$	$0.0000-0.0000j$	$0.9967-0.0368j$	$0.0000+0.0000j$	$0.0000-0.0000j$	$0.0033+0.0368j$
TM_{02}	$0.0000-0.0000j$	$-0.0000-0.0000j$	$0.0001-0.0002j$	$0.0000-0.0000j$	$0.0000+0.0000j$	$0.0000-0.0000j$	$0.0000+0.0000j$	$0.9975-0.0699j$	$0.0000-0.0000j$	$-0.0000-0.0000j$
TE_{12}	$-0.0000+0.0000j$	$0.0316-0.0031j$	$0.0000+0.0000j$	$-0.0000+0.0000j$	$-0.0316+0.0031j$	$-0.0010+0.0019j$	$-0.0000+0.0000j$	$-0.0000+0.0000j$	$0.9990+0.0019j$	$0.0000-0.0000j$
TM_{12}	$0.0434-0.0017j$	$0.0000+0.0000j$	$0.0001-0.0001j$	$0.0434-0.0017j$	$-0.0000-0.0000j$	$-0.0000+0.0000j$	$0.0033+0.0368j$	$-0.0000-0.0000j$	$-0.0000+0.0000j$	$0.9967-0.0368j$

Fig. 4. S-matrix of the bow-tie antenna obtained using the two methods, which give almost the same results.

TABLE I
EIGENVALUES OF CHARACTERISTIC MODES AND AMPLITUDES OF DOMINANT SPHERICAL WAVES GENERATED BY CHARACTERISTIC CURRENTS FOR A DIPOLE ANTENNA

Mode Number	Eigenvalue	Dominant Spherical Wave	Amplitude
1	0.427	TM_{02}	– 0.398
		TM_{04}	0.769
		TM_{06}	0.376
2	2.358	TM_{03}	0.874
		TM_{05}	0.430
3	2.452	TM_{01}	– 0.980
4	2.475	TM_{02}	– 0.880
		TM_{04}	– 0.429
5	– 18.364	TM_{03}	– 0.331
		TM_{05}	0.695
		TM_{07}	0.285

TABLE II
EIGENVALUES OF CHARACTERISTIC MODES AND AMPLITUDES OF DOMINANT SPHERICAL WAVES GENERATED BY CHARACTERISTIC CURRENTS FOR A BOW-TIE ANTENNA

Mode Number	Eigenvalue	Dominant Spherical Wave	Amplitude
1	1.511	TM_{01}	0.998
2	-9.028	TM_{-11}	– 0.670
		TM_{11}	0.670
		TE_{-12}	$-0.195j$
		TE_{12}	$-0.195j$
3	-14.908	TE_{-11}	$-0.396j$
		TE_{11}	$-0.396j$
		TM_{-12}	– 0.582
		TM_{12}	0.582
4	-28.245	TM_{02}	0.994
5	35.691	TE_{-11}	$-0.575j$
		TE_{11}	$-0.575j$
		TM_{-12}	0.389
		TM_{12}	– 0.389

We calculated the impedance matrix for the dipole antenna using a pulse function for the expansion and point matching for testing [11]. For the bow-tie antenna, we extracted the impedance matrix using the EM simulator FEKO, which uses an RWG basis function [12]. When we calculated the $\mathbf{S}$ using the first method, we connected loads of 500 Ω and 100 Ω to the feed gap of the dipole antenna and the bow-tie antenna, respectively. When we calculated the $\mathbf{S}$ using (25), we used the characteristic modes for which the eigenvalues and eigenvectors are real. We truncated the number of characteristic modes so that the $\mathbf{S}$ was convergent. We used eight dominant characteristic modes for the dipole antenna and six dominant characteristic modes for the bow-tie antenna.

Tables I and II show the eigenvalues of several low order characteristic modes and the amplitudes of the dominant spherical waves that each characteristic mode generates. Fig. 3 shows the $\mathbf{S}$ calculated using the two methods for the dipole antenna, and Fig. 4 shows the $\mathbf{S}$ calculated using the two methods for the bow-tie antenna. We show the dominant spherical waves in $\mathbf{S}$ in Figs. 3 and 4. The two results are almost the same, which shows the validity of the proposed method to determine the generalized scattering matrix.

VII. CONCLUSION

We derived a formula that calculates the generalized scattering matrix for an antenna. Once the characteristic currents flowing at a feed point, the amplitudes of the spherical waves produced by characteristic currents, and the eigenvalues of characteristic modes are known, the generalized scattering matrix can be determined. From the formula presented in this communication, we demonstrated that an antenna whose behavior is dominated by a single characteristic mode can be an MS antenna.

REFERENCES

[1] W. Wasylkiwskyj and W. K. Kahn, "Scattering properties and mutual coupling of antennas with prescribed radiation pattern," *IEEE Trans. Antennas Propag.*, vol. 18, no. 6, pp. 741–752, Nov. 1970.

[2] J. E. Hansen, *Spherical Near-Field Antenna Measurements*. London, U.K.: Peter Peregrinus, 1988.

[3] J. Rubio, M. A. Gaonzalez, and J. Zapata, "Generalized-scattering-matrix analysis of a class of finite arrays of coupled antennas by using 3-D FEM and spherical mode expansion," *IEEE Trans. Antennas Propag.*, vol. 53, no. 3, pp. 1133–1144, Mar. 2005.
[4] R. J. Garbacz and R. H. Turpin, "A generalized expansion for radiated and scattered fields," *IEEE Trans. Antennas Propag.*, vol. 19, no. 3, pp. 348–358, May 1971.
[5] R. F. Harrington and J. R. Mautz, "Theory of characteristic modes for conducting bodies," *IEEE Trans. Antennas Propag.*, vol. 19, no. 5, pp. 622–628, Sep. 1971.
[6] R. F. Harrington and J. R. Mautz, "Computation of characteristic modes for conducting bodies," *IEEE Trans. Antennas Propag.*, vol. 19, no. 5, pp. 629–639, Sep. 1971.
[7] R. F. Harrington, J. R. Mautz, and Y. Chang, "Characteristic modes for dielectric and magnetic bodies," *IEEE Trans. Antennas Propag.*, vol. 20, no. 2, pp. 194–198, Mar. 1972.
[8] W. K. Kahn and H. Kurss, "Minimum-scattering antennas," *IEEE Trans. Antennas Propag.*, vol. 13, no. 5, pp. 671–675, Sep. 1965.
[9] P. G. Rogers, "Application of the minimum scattering antenna theory to mismatched antennas," *IEEE Trans. Antennas Propag.*, vol. 34, no. 10, pp. 1223–1228, Oct. 1986.
[10] J. Rubio and J. F. Izquierdo, "Relation between the array pattern approach in terms of coupling coefficients and minimum scattering antennas," *IEEE Trans. Antennas Propag.*, vol. 59, no. 7, pp. 2532–2537, Jul. 2011.
[11] R. F. Harrington, *Field Computation by Moment Methods*. New York, NY, USA: MacMillan, 1968.
[12] S. M. Rao, D. R. Wilton, and A. W. Glisson, "Electromagnetic scattering by surfaces of arbitrary shape," *IEEE Trans. Antennas Propag.*, vol. 30, no. 3, pp. 409–418, May 1982.

A Koch-Shaped Log-Periodic Dipole Array (LPDA) Antenna for Universal Ultra-High-Frequency (UHF) Radio Frequency Identification (RFID) Handheld Reader

Heng-Tung Hsu and Ting-Jui Huang

***Abstract*—In this communication, we propose a printed log-periodic dipole array (LPDA) antenna covering the universal ultra-high-frequency (UHF) radio frequency identification (RFID) band of operation. Koch-shaped dipoles together with closely-coupled parasitic elements as directors were utilized for compactness in size and improvement in front-to-back ratio (F/B ratio). The experimental results demonstrate that the proposed antenna features good impedance match, moderate gain, better than 80% total radiation efficiency and excellent front-to-back ratio over the universal UHF RFID band from 840 MHz to 960 MHz. The antenna is well suitable for applications in RFID handheld readers.**

***Index Terms*—Antenna, array, dipole, log-periodic, radio frequency identification (RFID), ultra-high-frequency (UHF).**

I. Introduction

Passive radio frequency identification (RFID) system at UHF band has been popular due to the relatively long read range compared to systems operating at other frequencies. The breakthrough in technology has reduced the component cost substantially which helps to accomplish large-scale deployment such as item level tracking in warehouse management [1], [2]. In terms of the operating frequency, each country has its own allocation at UHF band as outlined in [3], leading to an overall coverage from 840 MHz to 960 MHz. For practical implementation cases, it is thus beneficial to have a universal antenna design covering the entire UHF band.

Antenna design has been an attractive research topic due to its importance in the highly application-oriented RFID systems. Over the past years, tag antenna designs have received considerable attention due to the variations in the object tagged [4]–[9]. Comparatively, antenna design on the reader side seemed much more straightforward because of the simplicity in the surrounding environment. Stacked patch radiators with novel feeding structure were utilized to achieve good antenna performance over the entire UHF RFID frequency bands in [3].

Despite the superior performance, the overall antenna size prohibits its integration into handheld readers.

The antenna design for handheld reader applications should meet certain requirements different from those for fixed reader antennas. One of the most challenging issues is the compactness in size while retaining good antenna characteristics at the same time. Additionally, the antenna should provide as much gain to save the battery life by reducing the RF output power under regulated maximum allowable EIRP. A high front-to-back ratio is also desired for handheld applications to reduce the absorption of electromagnetic energy by users. Detailed summaries for the characteristics of handheld reader antennas can be found in [10].

Over the past, various antenna configurations have been used for handheld applications. Printed dipole with parasitic elements placed in close proximity to the driven dipole was used in [11] to achieve averaged 4-dBi gain and 10-dB F/B ratio from 902 to 928 MHz. The antenna realized by 3-element Yagi configuration in [12] demonstrated a very high gain of 6 dBi and 1.3:1 VSWR with external impedance matching network covering 50 MHz bandwidth. Replacement of the matching network adjusted the operation band accordingly. A very recent publication [13] adopted crossed dipole antenna with proper phase offset and exhibited an 11.8% impedance bandwidth and 3.3% 3-dB axial-ratio bandwidth centered at 925 MHz with 1.0 dBi gain. To date, there has not been any handheld reader antenna design covering the universal UHF band ever reported in the open literature.

The LPDA configuration is probably the only candidate to meet all the electrical requirements over the entire UHF band for RFID applications. However, the overall size makes it difficult to be integrated into handheld readers. Though size reduction techniques have been proposed, the degradations in performance have to be tolerated [14]. Thus the main task of this communication is to achieve an antenna design to deliver comparable electrical performance as LPDA with reduced size. The proposed antenna is based on the LPDA configuration with Koch curves of the first iteration applied for size reduction purpose. Closely-coupled parasitic elements acting as directors were also included to improve the front-to-back ratio. The antenna configuration, design methodology, simulated and experimental results will be discussed in detail in the following sections.

II. Antenna Configuration

Fig. 1(a) shows the configuration and parameter definitions of the proposed antenna. The antenna was fabricated on both sides of the 1.6-mm-thick FR4 substrate with a dielectric constant $\varepsilon_r = 4.2$ and loss tangent $\tan\delta = 0.025$. Fig. 1(b) shows the picture of the fabricated prototype. The antenna is designed to cover the universal UHF RFID band from 840 MHz to 960 MHz. The proposed antenna adopts

Manuscript received June 06, 2012; revised April 10, 2013; accepted May 07, 2013. Date of publication May 21, 2013; date of current version August 30, 2013.

The authors are with the Department of Communications Engineering, Yuan Ze University, Taiwan, Republic of China (e-mail: htbeckhsu@saturn.yzu.edu.tw).

Color versions of one or more of the figures in this communication are available online at http://ieeexplore.ieee.org.

Digital Object Identifier 10.1109/TAP.2013.2264451